THE BEHAVIOR OF A PILE UNDER CYCLIC LATERAL LOAD

Kikuo Kotoda *
Satoru Kazama *
Presenting Author : Satoru Kazama

SUMMARY

By the results of cyclic lateral loading tests on many piles of different kinds of material, it has been made clear, especially for the reinforced concrete piles, that the effect of decreasing bending moment rigidity of piles as well as plasticity of subgrade reaction on the behavior of piles subjected to cyclic lateral load should not be overlooked.

In this paper, authors present a method to estimate the behavior of piles subjected to cyclic lateral load, in which the nonlinearity of bending rigidity of piles and also that of the subgrade reaction have been taken into account carefully.

INTRODUCTION

Recently, in order to mitigate as possible the noise and vibration due to pile driving, the bored reinforced concrete piles of large diameter made of cast-in-place concrete have been prevalently used, especially in urban areas in Japan. When piles of this kind are subjected to cyclic lateral load in case of earthquake, the behavior of these piles is considered to be complicated than that of piles made of elastic material such as steel piles. Actually, with the increase in intensity and repeating number of load in the tests, the bending rigidity of bored cast-in-place pile decreases gradually due to plastic property of materials of pile and remarkably due to tension cracks formed in piles.

At the beginning of this paper, we defined the load such that the load which was applied in the virgin stage in each test as the virgin load, and the load which was decreased until an unloading and reloaded in the succeeding stage as the repeated load.

METHOD OF ANALYZING THE BEHAVIOR OF PILE UNDER CYCLIC LOAD

In our analysis-model, both pile and ground are sliced into multi-thin layers as shown in Fig.1, in order to make it possible to get calculated values of both displacement and stress of pile which fit to actual values more precisely. The basic equations for displacement and stress of pile in arbitrary contiguous i-th and k-th layers are expressed as

$$\begin{aligned} &\text{i-th layer upper ground surface :} \quad {}_iEI(M_i)\frac{d^4y_i}{dx_i^4} = 0 \\ &\text{k-th layer under ground surface :} \quad {}_kEI(M_k)\frac{d^4y_k}{dx_k^4} + {}_kQ(X_k,y_k) = 0 \end{aligned} \tag{1}$$

where, x is the depth measured from the upper boundary of each layer, y is the displacement at depth x, and X is the depth from the ground surface to the upper boundary of each layer.

* Professor of Sc. & Eng. Res. Lab., Waseda Univ., Japan

Bending moment rigidity, EI(M), of each layer in Eq.1 is given as a function of the resistance moment(M) of a pile-section, which will be obtained by the calculation method mentioned later. Further, the subgrade reaction of soil, Q(X,y), of each layer is defined by Eq.2, which is obtained from many pile tests under cyclic load. The detail of the method will be mentioned later.

$$\text{For virgin load} \quad : \quad {}_kQ(X_k,y_k) = {}_kE_{s1}y_k = \frac{{}_kE_{s1}(X_k)\ y_k}{\sqrt{0.35\ y_k^2 + 0.6\ y_k + 0.05}}, \tag{2-a}$$

$$\text{For repeated load} \quad : \quad {}_k\bar{Q}(X_k,y_k) = {}_kE_{s1}\bar{y}_k = \frac{{}_kE_{s1}(X_k)\ \bar{y}_k}{\sqrt{0.35(\bar{y}_k/2)^2 + 0.6(\bar{y}_k/2) + 0.05}} \tag{2-b}$$

where, the coordinates under virgin and repeated load are taken as will be illustrated later in Fig.5. Therefore, in the case of the repeated load, y in Eq.1 may be transformed into $\bar{y}$.

Assuming that both EI(M) and Q(X,y) in each layer are constant, the general solutions for Eq.1 can be given as follows :

$$\text{i-th layer} : y_i = A_i + B_ix_i + C_ix_i^2 + D_ix_i^3 \tag{3-a}$$

$$\text{k-th layer} : y_k = e^{\beta_k x_k}(A_k\cos\beta_k x_k + B_k\sin\beta_k x_k) + e^{-\beta_k x_k}(C_k\cos\beta_k x_k + D_k\sin\beta_k x_k) \tag{3-b}$$

in which, $\beta_k = \sqrt[4]{E_s/EI}$, and A ~ D are arbitrary constants. These constants are determined by applying the boundary conditions at both head and tip of pile, and also from the continuity conditions between each layer.

The actual calculation of pile mentioned above is made by applying double convergence calculation with respect to M and y. The flow-chart is shown in Fig.2.

NONLINEARITY OF HORIZONTAL SUBGRADE REACTION OF SOIL UNDER VIRGIN LOAD AND REPEATED LOAD

The nonlinearity of horizontal subgrade reaction of soil in this study is evaluated in the following way from the results of many lateral loading tests of pile.

The basic equation of pile subjected to a lateral load can be expressed in Eq.4, (Fig.3).

$$EI\frac{d^4y}{dx^4} + E_s\ y = 0 \tag{4}$$

where, EI : bending rigidiy of pile-section
E_s : modulus of horizontal subgrade reaction of soil
x, y : depth from ground surface and displacement of pile at depth x, respectively

As has been recoganized in the results of many pile tests, the value of E_s becomes smaller as the displacement of pile becomes larger. Thereupon, we have reckoned backward the value of E_s by applying the solution of Eq.4 into the results of many pile tests and made clear the nonlinearity of E_s under both virgin and repeated load. To distinguish $\bar{E}_s$ under the repeated load from E_s under the virgin load, in the calculation of $\bar{E}_s$, the new coordinates which refer to lateral load($\bar{H}$) and displacement($\bar{y}$) are established as shown in Fig.3.

Further, in order to make more clear the nonlinearity of E_s and $\bar{E}_s$ so far obtained, these values which correspond to arbitrary value of displacement(y, $\bar{y}$) are divided by the value of E_{s1} determined for y=1 cm under the virgin load applied in each test.

In Fig.4, are shown the results calculated by the processes mentioned above, that is, the relationships between E_s/E_{s1} and y under the virgin load, and $\bar{E}_s/E_{s1}$ and $\bar{y}$ under the repeated load. From these results, it may be said that the nonlinearity of the modulus of subgrade reaction of soil under both virgin and repeated load is given as a function of the displacement of pile. Considering these results, we tried to establish the expressions for estimating the nonlinearities of E_s/E_{s1} and $\bar{E}_s/E_{s1}$, with a results of the following equations which we want to propose for this purpose.

$$\text{For virgin load} : \frac{E_s}{E_{s1}} = \frac{1}{\sqrt{0.35\ y^2 + 0.6\ y + 0.05}} \tag{5-a}$$

$$\text{For repeated load} : \frac{\bar{E}_s}{E_{s1}} = \frac{1}{\sqrt{0.35\ (\bar{y}/2)^2 + 0.6\ (\bar{y}/2) + 0.05}} \tag{5-b}$$

The equations obtained above are applied in the calculation of pile in this paper, as shown in Eq.1 and Eq.2 mentioned before. Further, in Fig.5, are shown the relationships between Q/E_{s1} and y under the virgin load, and $\bar{Q}/E_{s1}$ and $\bar{y}$ under the repeated load, which are deduced from Eq.5.

NONLINEARITY OF BENDING RIGIDITY OF PILE

In the calculation of the bending rigidity of pile, EI(M) in Eq.1, the effect of tension cracks which occur in concrete and the tensile strength of concrete are especially considered in addition to the plastic property of concrete and steel bar. The strain distribution in a pile cross-section is assumed as linear, as shown in Fig.6. The stress distribution of concrete and steel bars which corresponds to the strain distribution is determined as will be shown later in Fig.9.

In Fig.7 is shown the flow chart of the process of calculating the bending rigidity, EI(M), which is a function of the bending moment, M.

HORIZONTAL BEHAVIOR OF A CAST-IN-PLACE REINFORCED CONCRETE PILE UNDER CYCLIC LOAD

In this paper, the analysis was made for a cast-in-place reinforced concrete pile which was tested under the cyclic lateral load. This pile was driven in deep soft ground as shown in Fig.8. The upper part of pile is larger than the lower part in diameter. At the time of cyclic loading tests, the condition of pile head was free. The horizontal displacement of pile head and strain in steel bars at various depths were measured by means of the dialguages and strain gauges, respectively.

In the calculation of the horizontal behavior of the pile tested above, both pile and soil were sliced into 15-thin layers. The value of E_{s1} of each layer in Fig.2 was increased with increasing depth from the ground surface as shown in Fig.8(c).

The stress-strain curves of concrete and steel bar, which were used in the calculation of EI(M) mentioned before, were determined as shown in Fig.9, considering the results obtained from the tests of concrete cores and steel bars. In Fig.10, are shown the calculated relations between EI(M) and M for each cross-section(sections I IV, in Fig.8(b)). It will be noticed that EI(M) is affected extremely by the tension cracks formed in concrete, and the value decreases to one-fifth of the value in the state of non-crack-formation. As for the resisting moment, M, the value decreases temporarily by crack formation in concrete, but the value increases thereafter. From the results of calculation made for the tested pile as mentioned below, it is recoganized that the actual behavior of pile does not follow the EI-M curve always, especially when M decreases temporarily.

The calculations were made for two cases of tested pile, i.e., (i) CASE I : assuming the concrete and steel bars of pile material be in elastic range, and (ii) CASE II : considering the crack formation in concrete in addition to the nonlinearity of concrete and steel bars as shown in Fig.9.

In Fig.11(a) are shown the hysteresis loops of pile behavior, which are calculated by applying the assumption in CASE I, in a comparision with those obtained actually by the test. A similar comparision made for CASE II is shown in Fig.11(b). The displacement of the calculated hysteresis loops of CASE I becomes smaller as the cyclic load becomes larger, as compared with that in the test results. For this reason, the crack formation in concrete is not considered in the calculation especially. On the other hand, it may be said that the hysteresis loops calculated for CASE II coinside with the test results, in both shape and value of the curves. Further, it will be recoganized from the results both tested and calculated that the cracks are formed in concrete at about 60 tons of lateral load and the displacement of pile increases extremely from this extent of load.

Fig.12 shows the strain distributions in steel bars, which are calculated for CASE II at the maximum lateral load in each cycle, for a comparison with the measured distributions. From this figure, it may be said that the calculated distributions show a good agreement with those measured, and the maximum strain on the tension side becomes larger as lateral load increases, as well as the displacement mentioned above, especially after the crack formation in coccrete.

CONCLUSION

From the above results, the calculation method, which is proposed in this paper, may be said to be available for the estimation of horizontal behavior of reinforced concrete pile subjected to cyclic load in case of earthquake.

REFERENCES

1. Kotoda, K. and Kazama, S. : Calculating method of Lateral Loading Pile, Tsuchi To Kiso, J.S.S.M.F.E., Vol.25,No.8, 1978
2. Takeuchi, M., Kotoda, K. and Kazama, S. : Lateral Behavior of A Pile under Cyclic Load, Summaries of Technical paper, Annual Meeting of A.I.J., 1980

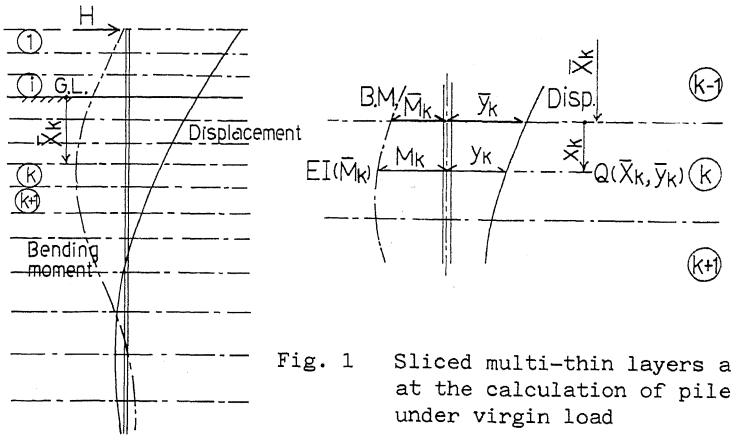

Fig. 1 Sliced multi-thin layers and coordinates at the calculation of pile behavior under virgin load

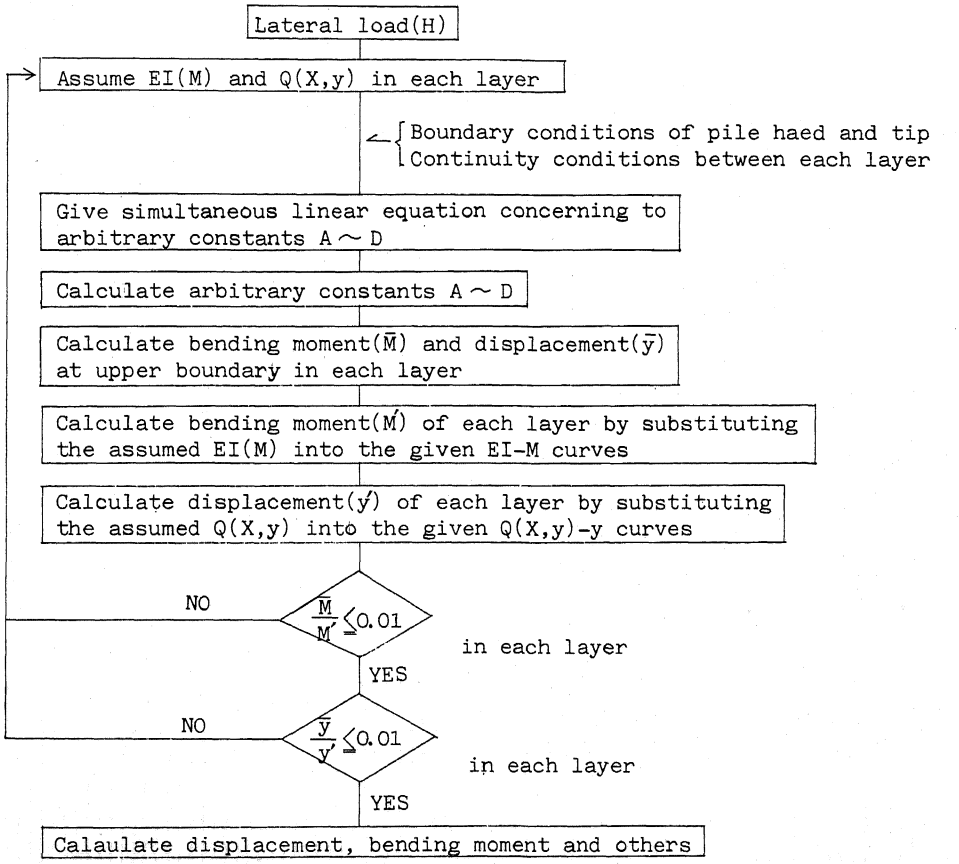

Fig. 2 Flow chart of the calculation of pile behavior under cyclic load

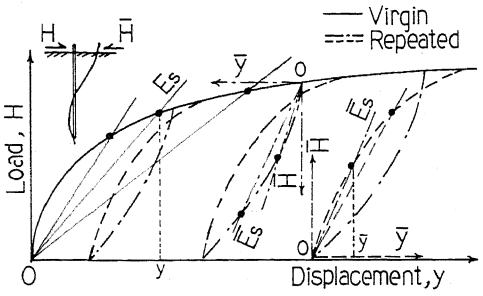

Fig. 3 Calculation of E_s and E_s from test results of pile under cyclic load, and coordinates at the calculation

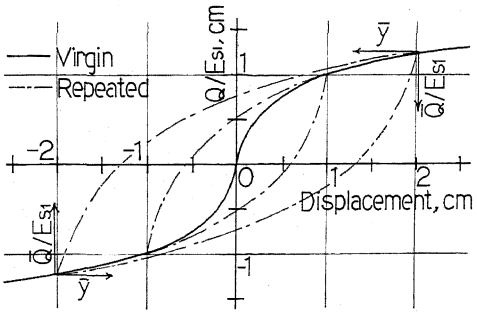

Fig. 5 Q/E_{s1}-y curve and Q/E_{s1}-y curve determined by Eq.(5-a) and Eq.(5-b), respectively

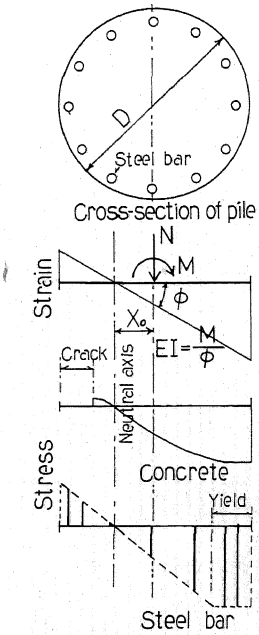

Fig. 6 Strain and stress distributions at the calculation of bending rigidity(EI) of pile cross-section

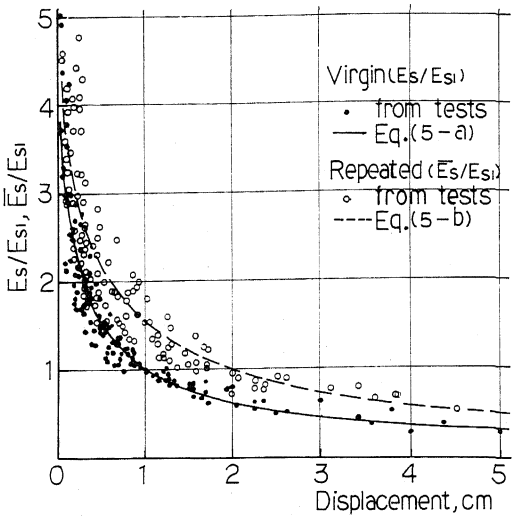

Fig. 4 E_s/E_{s1}-y curve under virgin state and E_s/E_{s1}-y curve under repeated state, obtained from many test results of pile

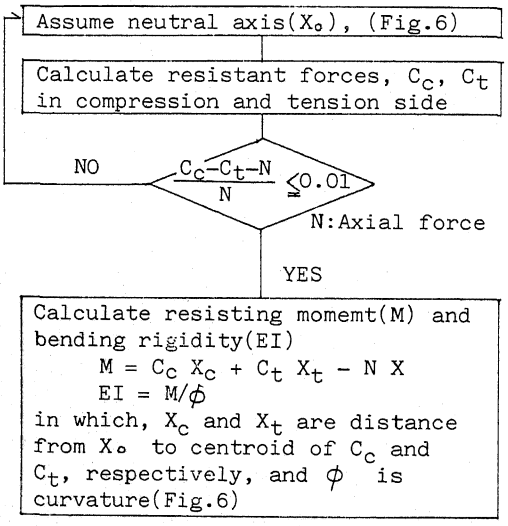

Fig. 7 Flow chart of the calculation of EI and M

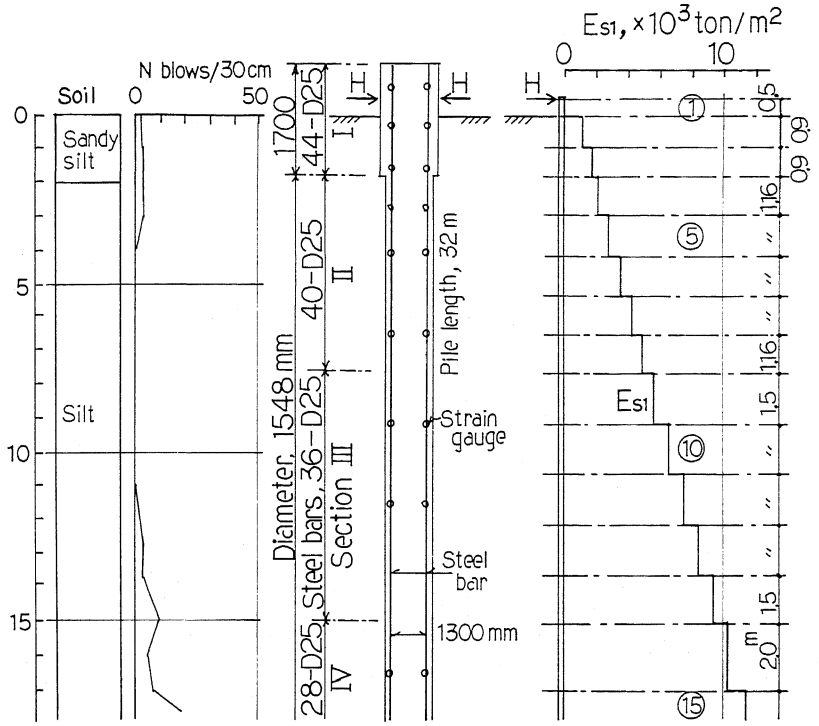

(a) Boring log (b) Tested pile (c) Sliced layers and E_{s1}

Fig. 8 Cast-in-place reinforced concrete pile which was tested under cyclic load, and sliced layers and E_{s1}-value applied on the calculation of pile behavior

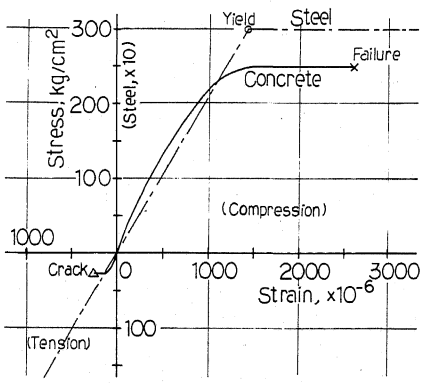

Fig. 9 Stress-strain curves of concrete and steel bar used on the calculation of bending rigidity(EI)

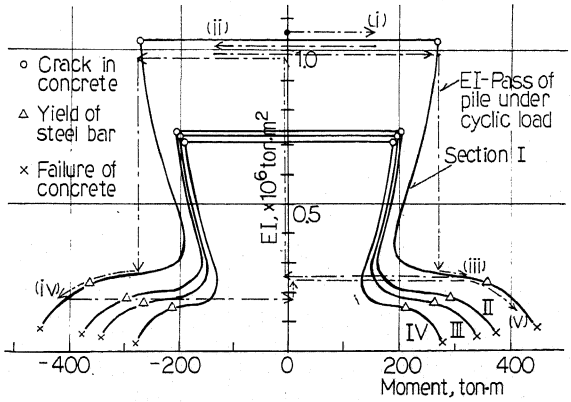

Fig. 10 Relationships between EI and M, which were calculated by applying the values shown in Fig.9, of each cross-section of pile(Fig.8)

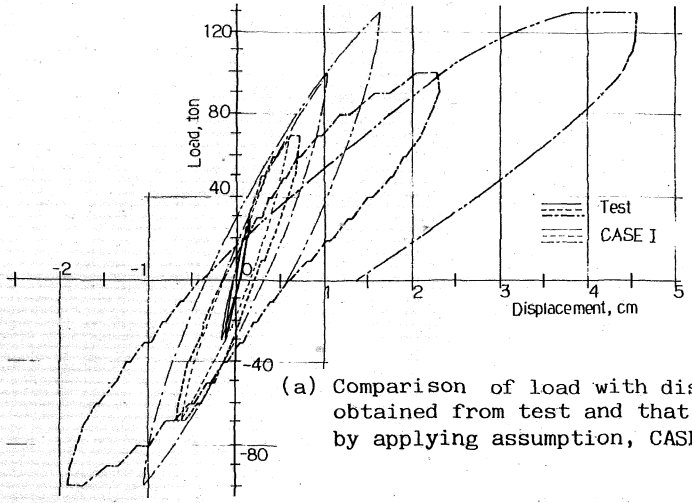

(a) Comparison of load with displacement, obtained from test and that calculated by applying assumption, CASE I

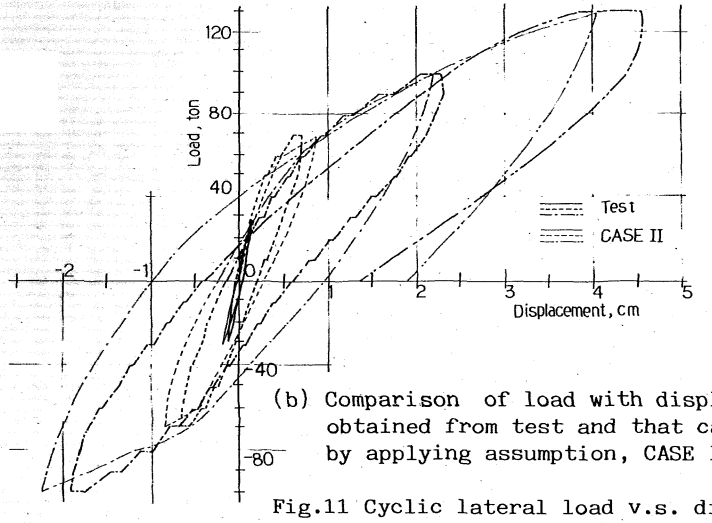

(b) Comparison of load with displacement, obtained from test and that calculated by applying assumption, CASE II

Fig.11 Cyclic lateral load v.s. displacement

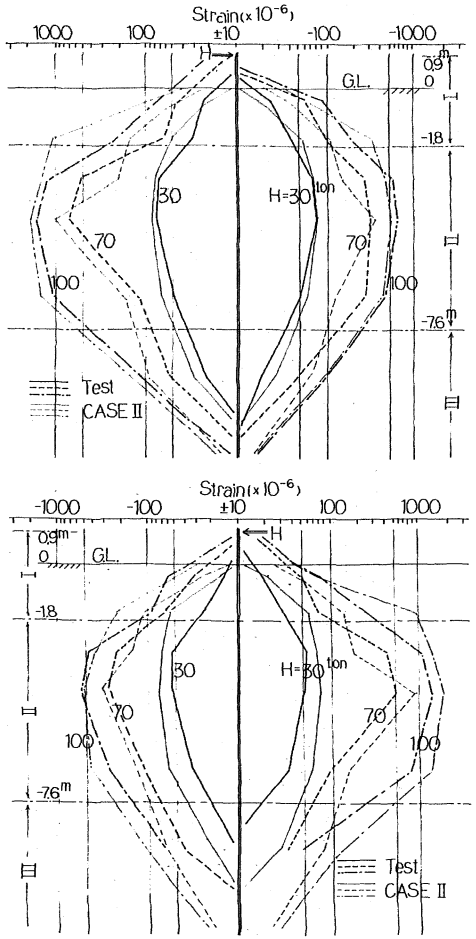

Fig.12 Measured and calculated strain distribution in steel bar